



Kinetic study of lead (Pb²⁺) removal from battery manufacturing wastewater using bagasse biochar as biosorbent

Poonam¹ · Sushil Kumar Bharti¹ · Narendra Kumar¹

Received: 8 March 2018 / Accepted: 2 July 2018 / Published online: 10 July 2018
© The Author(s) 2018

Abstract

Agricultural waste of bagasse was employed for investigating its lead (Pb²⁺) removal potential from wastewater of battery manufacturing industry. To optimize maximum removal efficacy of the bagasse, it was thermally modified in the form of biochar. Adsorption kinetics and mechanism including various parameters (contact time, dose and pH) were studied employing biochar prepared from bagasse waste. The optimum adsorption occurred at pH 5 with 140 min. of contact time utilizing 5 g of adsorbent dosage at room temperature (25 ± 3 °C). The maximum removal efficiency was recorded as 12.741 mg g⁻¹ with 75.376% of removal at optimum pH 5 as compared to the initial concentration in the effluent. The result illustrated the most suitable fit was for Langmuir isotherm with monolayer and homogenous adsorption of Pb²⁺. The kinetics involved in the process was observed to be pseudo-second-order, which indicates chemisorption as a major phenomenon involved in the process. The characterization of the adsorbent biochar was done by SEM, EDX and FTIR analysis that provided details about ultrastructural and functionality of organic moiety present to have porous and rough surface, favoring the adsorption process. The functional groups identified by the FTIR analysis demonstrated involvement of carboxyl groups in Pb²⁺ binding. Postadsorption elution of metal-loaded bagasse was executed by 0.1 M HNO₃ with about 90% of regeneration.

Keywords Biosorption · Biochar · Isotherms · Kinetics · Desorption · Water pollution · Heavy metals

Introduction

Industrialization and urbanization have all the limits to sustain a healthy and peaceful life on the earth (Li et al. 2017). Among them, aquatic pollution caused by release of various heavy metals (HMs) from different anthropogenic activities is one of the major environmental concerns (Amuda et al. 2007; Ajenifuja et al. 2017). These HMs have the bioaccumulation tendency, non-biodegradable nature and may contaminate the food chain threatening the existence of living beings (Rangabhashiyam and Selvaraju 2015; Poonam and Kumar 2018).

Lead (Pb²⁺) is one of the most toxic HMs, as lowest concentration in drinking water may cause serious problems to the nervous and reproductive system, kidney, liver, brain and bony tissues (Renner 2010; Andrade et al. 2015). The recommended concentration level of by the Environmental Protection Agency (EPA) is 0.015 and 0.05 mg l⁻¹ in drinking and wastewater, respectively (Salmani et al. 2017; Gil et al. 2018). The main sources of the Pb²⁺ pollution are battery manufacturing industry, shooting ranges, paint industries, mining processes, chemical manufacturers, surfactants, preservatives, etc. (Xu et al. 2013; Liu et al. 2016; Laidlaw et al. 2017; Mehmood et al. 2017). The removal of Pb²⁺ from wastewater is accomplished by various conventional techniques like precipitation with hydroxide ion or lime, ion exchange, coagulation, electrochemical process, reverse osmosis and ion flotation (Wang and Chen 2009; Kong et al. 2014; Ehrampoush et al. 2015). But, these methods are expensive as well as produce secondary wastes such as persistent organic pollutants, volatile organic compounds (Salmani et al. 2017; Banerjee et al. 2012). Therefore, one of the most effective and low-cost techniques, adsorption, has attracted researchers for the removal of HMs from

✉ Narendra Kumar
narendrakumar_lko@yahoo.co.in

Poonam
poonam.rgnp@gmail.com

Sushil Kumar Bharti
bhartisushil93@gmail.com

¹ Department of Environmental Science, Babasaheb Bhimrao Ambedkar University, Raebareli Road, Lucknow, UP 226025, India

water bodies (Trans et al. 2010; Uçar et al. 2015). However, modification of adsorbents for better performance may be a restricting factor in view of consumption of energy and chemicals (Gil et al. 2018). Till now available studies suggest the use of readily available and cheaper materials for example agricultural wastes, industrial wastes and household wastes, algae and fungi for the removal of Pb^{2+} from water (Saka et al. 2011; Taha et al. 2011; Ibrahim et al. 2012; Reddy et al. 2014; Cheraghi et al. 2015).

Various researchers have used the by-product of sugarcane, i.e., bagasse adsorption of different pollutants including heavy metals, dyes (Joseph et al. 2009; Saad et al. 2010; Said et al. 2013; Gardare et al. 2015; Abdelhafez and Li 2016; Tahir et al. 2016). It is an easily available waste which can be collected from different sugar mills and juice shops. In the present study bagasse was used as adsorbent for the purpose of removal of Pb^{2+} from battery manufacturing industry effluent. The adsorbent was thermally modified into biochar to enhance the efficiency of adsorbent as thermal treatment increased the surface area and porosity of the adsorbent (Doke and Khan 2017). Adsorption is a surface phenomenon which depends on a number of parameters like pH, contact time, adsorbent dose, initial metal concentration, pore size, temperature, surface area (Buasri et al. 2012; Nguyen et al. 2013; Salmani et al. 2017). The goal of the present study is to assess the effectiveness and performance of bagasse biochar for the removal of Pb^{2+} from wastewater of battery manufacturing industry effluent. Therefore, the effect of contact time and adsorbent dose on room temperature (25 ± 3 °C) and at pH 5 (optimized) was investigated to optimize the kinetics and isotherms involved in the process. The experiments were performed in batch technique, and adsorption capacity was calculated in the each step for the optimization of the parameters.

Materials and methods

Sample collection

Wastewater was collected from the effluent outlet of battery manufacturing industry situated near Aishbagh Park, Lucknow, UP. The samples were collected in sampling gallons of 10 l during winter season (January 2016) to minimize the influence of microbial activity on physicochemical properties of the wastewater which were examined by following methods of APHA (2005).

Adsorbent preparation

Bagasse was collected from sugar juice shops of Rajnikhand, Lucknow. After collection, it was brought to the laboratory and washed out thoroughly first with tap water after that

deionized water for removing dust and unwanted objects. Lastly, bagasse was air-dried for 2 weeks to remove the moisture content. Then, it was subjected to pyrolysis at temperature of about 300 ± 10 °C for 2.5 h. After cooling overnight, the biochar was washed thoroughly with deionized water to remove unwanted ash contents. Thereafter, it was dried in the oven and stored in desiccated condition in airtight containers.

Characterization of the adsorbent

All of the chemical reagents used in the present study were of analytical reagent (AR) grade from E. Merck, Darmstadt, Germany. The adsorbent was characterized by atomic adsorption spectrometer (AAS), Fourier transform infrared spectroscopy (FTIR), scanning electron microscope (SEM) and energy-dispersive X-ray analysis (EDX) studies. The concentration of Pb^{2+} was determined by AAS (Varian AA240FS). The functional groups present in the biochar before and after treating the wastewater were determined by FTIR (Nicolet™ 6700). Surface morphology was observed by SEM (JSM-6490LV, manufactured by JEOL, Japan) micrographs. Further, elemental composition was analyzed by EDX (model no. JSM-6490LV, designed by JEOL, Japan) and elemental composition (C, H, N and S %) was analyzed by CHNS analyzer (model no. Flash EA112 Series, manufactured by Thermo Finnegan). Surface area and pore size of bagasse biochar (before and after treatment) were characterized by Quanta Chrome Nova-1000 surface analyzer instrument under liquid N_2 temperature. Further, adsorption–desorption studies were performed in order to determine the evolution of porosity and textural properties and surface area from Brunauer–Emmett–Teller (BET) method. Barrett–Joyner–Halenda (BJH) method was used to evaluate pore diameter and volume and de Boer t-method for the newly generated micropore volume measurement (Venkatesha et al. 2016). The structural integrity of the sample was observed by powder X-ray diffraction (XRD). The data were recorded by step scanning at $2\theta = 0.0200/s$ from 30 to 800 on PANalytical X'Pert PRO MPD X-ray diffraction with graphite monochromatized Cu K α radiation ($\lambda = 0.15406$).

Quantitative evaluation of surface acidic functional groups on the adsorbent

The acidic functional groups present on the surface of biochar were determined by the following Boehm titration method (Boehm et al. 1964; Oickle et al. 2010). 0.05 M $NaHCO_3$, Na_2CO_3 and NaOH bases were used in this method. 0.5 g of adsorbent was added in 50 ml of three bases. After that, the samples along with blank were shaken for 24 h at 120 rpm and then filtered it to remove extra particles. Thereafter, 20 ml of filtrate from each one was titrated with 0.05 M HCl

to neutralize the base completely, and then backtitration was done by the blank solution with 0.05 M NaOH. The phenolphthalein indicator was used to determine the end point of the reaction. All titrations were carried out at room temperature (25 ± 3 °C), and the solutions were made up of Millipore water. The difference between molar NaOH and Na_2CO_3 was assumed to be the phenolic group content as described by Oickle (2010) and Abdelhafez and Li (2016).

Following steps were used to calculate different surface acidic groups

1. Calculation of surface acidic groups amount (A_x)

$$A_x = \frac{(V_{bx} - V_x) \cdot M_{\text{HCl}} \cdot 2.5}{m_x} \text{ mol g}^{-1}$$

where m_x = mass of biochar (gm), V_{bx} = volume (ml) of HCl used for the titration of blank, V_x = volume (ml) used for sample titration of respective bases solution after biochar addition, M_{HCl} = molarity of HCl concentration in moles/lit., 2.5 is a coefficient for decreasing titration sample volume in comparison with reaction sample volume (50 ml/20 ml),

2. Calculation of the amount of different kinds of surface groups
 - a. Amount of phenolic groups, $A_{\text{ph}} = A_3 - A_2 - A_1$
 - b. Amount of carboxylic groups, $A_{\text{ca}} = A_1$
 - c. Amount of carboxylic from lactones hydrolysis groups $A_{\text{la}} = A_2 - A_1$
where A_1 , A_2 and A_3 are amount of surface acidic groups for NaHCO_3 , Na_2CO_3 and NaOH, respectively.

Moisture and ash content

Moisture content: 1 g of sample was dried for 24 h in an oven at temperature of 100 ± 5 °C until constant weight was gained. Moisture content was calculated using the following formula

$$\text{Moisture content(\%)} = \frac{w_i - w_f}{W_i} \times 100$$

where w_i = initial weight of the adsorbent (gm), w_f = final weight of adsorbent after drying (gm).

Ash content: It was determined with the help of muffle furnace by weighing 1 g of the sample and placing it into a porcelain crucible. The crucible was heated up to 500 ± 5 °C for 5 h. The material was allowed to cool down in a desiccator for 15 min. The ash content was calculated by using the following formula

$$\text{Ash content(\%)} = \frac{W_2 - W_0}{W_1 - W_0} \times 100$$

where W_0 = weight of empty crucible (g), W_1 = weight of crucible (g) + weight of adsorbent (gm), W_2 = weight of crucible (g) + weight of ashed sample (g) (Basu et al. 2017; Poonam and Kumar 2018).

Experimental setup

The adsorption experiment was performed by varying adsorbent dosage from 2.0 to 5.0 g L^{-1} at an interval of 0.5 g, for 100 ml in 250-ml Erlenmeyer flasks at rotating speed of 120 rpm. The pH was optimized for maximum adsorption by shifting it from 2 to 5 with 0.1 N NaOH and 0.1 N HCl. The contact time was also optimized by varying it from 20 to 140 min at an interval of 20 min, until the maximum adsorption was achieved.

Adsorption rate kinetics

The adsorption kinetics involved is an important parameter to describe the basic traits of a good adsorbent (Wang et al. 2012). It provides the process which controls the sorbate reactions in the solid–solution interface at different time. The present study pseudo-first- and second-order reactions were utilized to describe the adsorption mechanism involved in the Pb^{2+} removal processes by bagasse biochar (Lagergren 1898; Ho et al. 2000).

The pseudo-first-order kinetic model (Eq. 1) is expressed as

$$\ln(q_1 - q_t) = \ln q_1 - k_1 t \quad (1)$$

where q_1 and q_t are the amount of Pb^{2+} (mg g^{-1}) adsorbed at equilibrium and at time t , respectively, and k_1 is the first-order rate constant (min^{-1}).

According to Mckay and Ho (1999), pseudo-second-order kinetic model (Eq. 2) is expressed as

$$\frac{t}{q_t} = \frac{1}{k_2 q_2^2} + \frac{1}{q_2} t \quad (2)$$

$$\frac{1}{q_t} = \frac{1}{K_2 q_2 t} + \frac{1}{q_2} \quad (3)$$

Equation (3), modified Ritchie's second-order kinetic model, is used to calculate the initial sorption rate, h ($\text{mg g}^{-1} \text{min}^{-1}$) (Eq. 4).

$$h = K_2 q_2^2 \quad (4)$$

where q_2 is the maximum adsorption capacity (mg g^{-1}) for the pseudo-second-order adsorption, K_2 is the equilibrium rate constant for the pseudo-second-order adsorption ($\text{g mg}^{-1} \text{min}^{-1}$), and h is initial sorption rate ($\text{mg g}^{-1} \text{min}^{-1}$).

Adsorption isotherm studies

The experimental uptake (q_e) values obtained from batch assay were analyzed using adsorption isotherm models (Langmuir and Freundlich) and separation factor (R_L) at room temperature (25 ± 3 °C) and other optimized conditions, i.e., pH 5, dose 5.0 g and 140 min of contact time.

The linear form of Freundlich adsorption isotherm is given as the following

$$\log q_e = \log K_f + \frac{1}{n} \log C_e$$

where K_f and n are Freundlich constants for distribution coefficient and intensity, respectively.

The Langmuir equation is given as

$$\frac{C_e}{q_e} = \frac{1}{q_{\max} K_L} + \frac{C_e}{q_{\max}}$$

where q_e is the equilibrium metal ion concentration, C_e is the equilibrium metal ion concentration in the solution (mg l^{-1}), q_{\max} is the monolayer adsorption capacity of bagasse biochar (mg g^{-1}), and K_L is the Langmuir adsorption constant (L mg^{-1}).

Analytical method

The amount of Pb^{2+} adsorbed was calculated by the following mass balance relationship

$$q_e = \frac{C_0 - C_e}{w} \times v$$

and percent removal at the equilibrium (q_e) was calculated as the following

$$\text{Removal(\%)} = \frac{(C_0 - C_e)}{C_0} \times 100$$

where C_0 and C_e (mg l^{-1}) are the metal concentrations at initial stage and equilibrium, respectively. v is the volume of the effluent in ml, and w is the weight of the adsorbent in grams(gm).

Desorption study

Desorption experiments were performed with metal-loaded biochar of bagasse to check the reusability of the adsorbent. 0.1 M HCl, HNO_3 and H_2SO_4 , and NaOH were used as desorbing eluants. One gram of the Pb^{2+} -loaded adsorbent was added in 100 ml of eluants and incubated for 3 h at 30 °C at 150 rpm.

Results and discussion

Physicochemical properties of battery manufacturing industry effluent

The physicochemical properties of battery manufacturing industry effluent are presented in Table 1. Most of the parameters were found to be beyond the limits prescribed in Bureau of Indian Standards (BIS 10500: 2012) for on land irrigation. pH, temperature and electrical conductivity (EC) affect the ionic concentration of the effluent and influence the chemical reactions in the aquatic environment (Akpomie and Dawodua 2015). Different salts, used in the processes, may be the reason for higher values of pH as well as EC. Chemical oxygen demand (COD), biological oxygen demand (BOD), dissolved oxygen (DO), total dissolved solids (TDS), total suspended solids (TSS) and total solids (TS) define the amount of pollution caused by different organic and inorganic pollutants affecting the water quality. Besides hardness and alkalinity higher concentration of nitrate, phosphate and sulfate may be attributed to the usage of different chemicals and salts during the battery manufacturing processes (Ahmed et al. 2012).

Table 1 Physicochemical properties of battery manufacturing industry effluent

S. no.	Parameters	Average \pm SD	BIS (10500:2012) On land for irrigation
1	Color	Transparent white	–
2	Odor	Light vinegar	Non-objectionable
3	Temperature	29.733 ± 0.208	–
4	pH	8.033 ± 0.208	5.5–9
5	EC	24.167 ± 0.751	–
6	BOD	2968.02 ± 29.197	100
7	COD	$12,500.50 \pm 165.751$	–
8	TDS	1455.333 ± 6.429	2100
9	TSS	757.333 ± 74.717	200
10	TS	2217.667 ± 4.028	2300
11	Acidity	583.333 ± 4.578	–
12	Alkalinity	400.00 ± 2.646	–
13	Chloride	140.413 ± 1.859	–
14	Sulfate	43.757 ± 3.174	–
15	Phosphate	67.5033 ± 1.402	–
16	Nitrate	nd	–
17	Total hardness (as CaCO_3)	621.00 ± 263.236	–
18	Lead (Pb^{2+})	2.393 ± 0.030	0.1

Results are expressed as mean of five replicates \pm SD (i.e., $n=3$); all the results were expressed in mg l^{-1} except for color, odor, pH, temperature (°C) and EC (Siemen m^{-1})

nd not detected

The concentration of Pb^{2+} in the effluent was found to be 2.393 mg l^{-1} which exceeded the limit of 0.1 mg l^{-1} as prescribed by BIS (10500: 2012). Higher concentration of Pb^{2+} in the water bodies may be harmful for health of flora and fauna (Babel and Kurniawan 2003; Alluri et al. 2007).

Screening of biosorbents

Three thermally modified agrowastes (biochar of bagasse, orange and coir) were observed for their suitability for adsorbing Pb^{2+} (Fig. 1). Among them, bagasse biochar showed maximum adsorptive removal of 75.38% Pb^{2+} in comparison with orange (70.36%) and coir (61.98%) for the same adsorbent dosage of 5.0 g l^{-1} . The variation in the adsorption efficiencies may be attributed to variations in the morphology and binding sites of the adsorbents (Petrović et al. 2017).

Characteristics of adsorbent

The proximate and ultimate study of the adsorbents is summarized in Table 2. The ash content was found to be low with average value of 7.337% because of the biochar-producing processes which eliminate the oxygen content. The moisture content was also found to be very low with average value of 1.968% which facilitated the adsorption process. The bagasse biochar was alkaline in nature as pH was found to be 8.967 which could be recognized by the detachment of alkali metal, i.e., Ca^{2+} as their concentration was found to be moderately high as shown in EDX spectrum of biochar (Fig. 2e). The surface area of the biochar ($12.378 \text{ m}^2 \text{ g}^{-1}$) seems to be rough and irregular which was confirmed by SEM image of bagasse biochar (Fig. 2b). Further, the biochar showed comparatively higher C/H and C/N ratio and less C % (Table 1) which suggests that the charring process was not accomplished well with some decomposed matter.

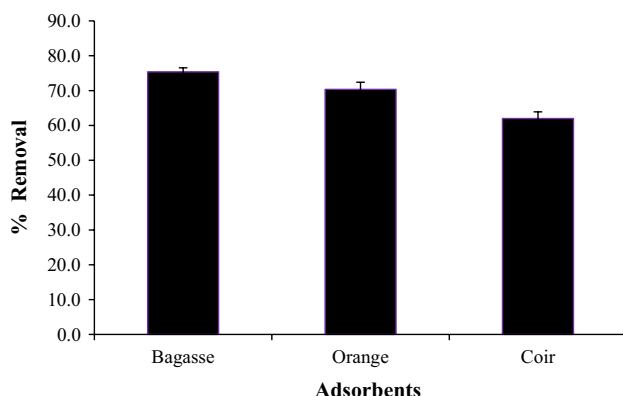


Fig. 1 Adsorption efficiency of different agrowastes at room temperature ($25 \pm 3 \text{ }^\circ\text{C}$), \pm SD shown by error bar

Table 2 Characteristics of bagasse biochar

S. no.	Characteristics	Values
1	Moisture content (%) ^a	1.968 ± 0.012
2	Ash content (%) ^a	7.337 ± 0.033
3	pH	9.267 ± 0.208
4	Pore volume (cc/g) ^b	0.039 ± 0.003
5	Pore diameter (nm) ^b	1.579 ± 0.023
6	Surface area (m^2/g) ^b	12.628 ± 0.30
7	C % ^c	38.153 ± 0.531
8	H % ^c	6.076 ± 0.038
9	O % ^{c*}	50.942 ± 0.215
10	N % ^c	4.557 ± 0.289
11	S % ^c	0.272 ± 0.010
12	C/H ratio ^c	6.314 ± 0.064
13	C/N ratio ^c	8.759 ± 0.002

^aData are presented as dry weight percent

^bData are retrieved from BET analysis

^cData are retrieved from CHNS analyzer

^{c*}Determined by difference

This may also be a reason for comparatively lesser specific surface area of the biochar as analyzed by BET. In addition to this, higher values of H and O % indicate availability of binding sites responsible for the successful adsorption of Pb^{2+} (Table 1). The results were found to be in good agreement with Fernandez et al. (2014); Abdelhafez and Li (2016); and Basu et al. (2017).

SEM and EDX

SEM and EDX images showed the change in the morphology of the adsorbent before and after adsorption process (Fig. 2). The differences in SEM image of (a) bagasse, (b) its biochar and (c) Pb^{2+} -loaded biochar could be clearly visualized. Before charring the surface was uniform and very smooth, and after thermal treatment, it became comparatively rough and irregular increasing the surface area. After adsorption, the space became filled with some irregular, crystalline structures which supported the adsorption of Pb^{2+} from the effluent. In addition to this, existence of Pb^{2+} in the EDX spectrum may also be considered in the support successful adsorption of the metal (Fig. 2d, e).

FTIR

Adsorption process is affected by the groups and bonds present in the adsorbent. In order to investigate the chemical structure and major functional groups present, which may be responsible for adsorption process, FTIR analysis was carried out (Solum et al. 1995). The spectra of the (a) bagasse, (b) its biochar and (c) Pb^{2+} -loaded biochar are presented

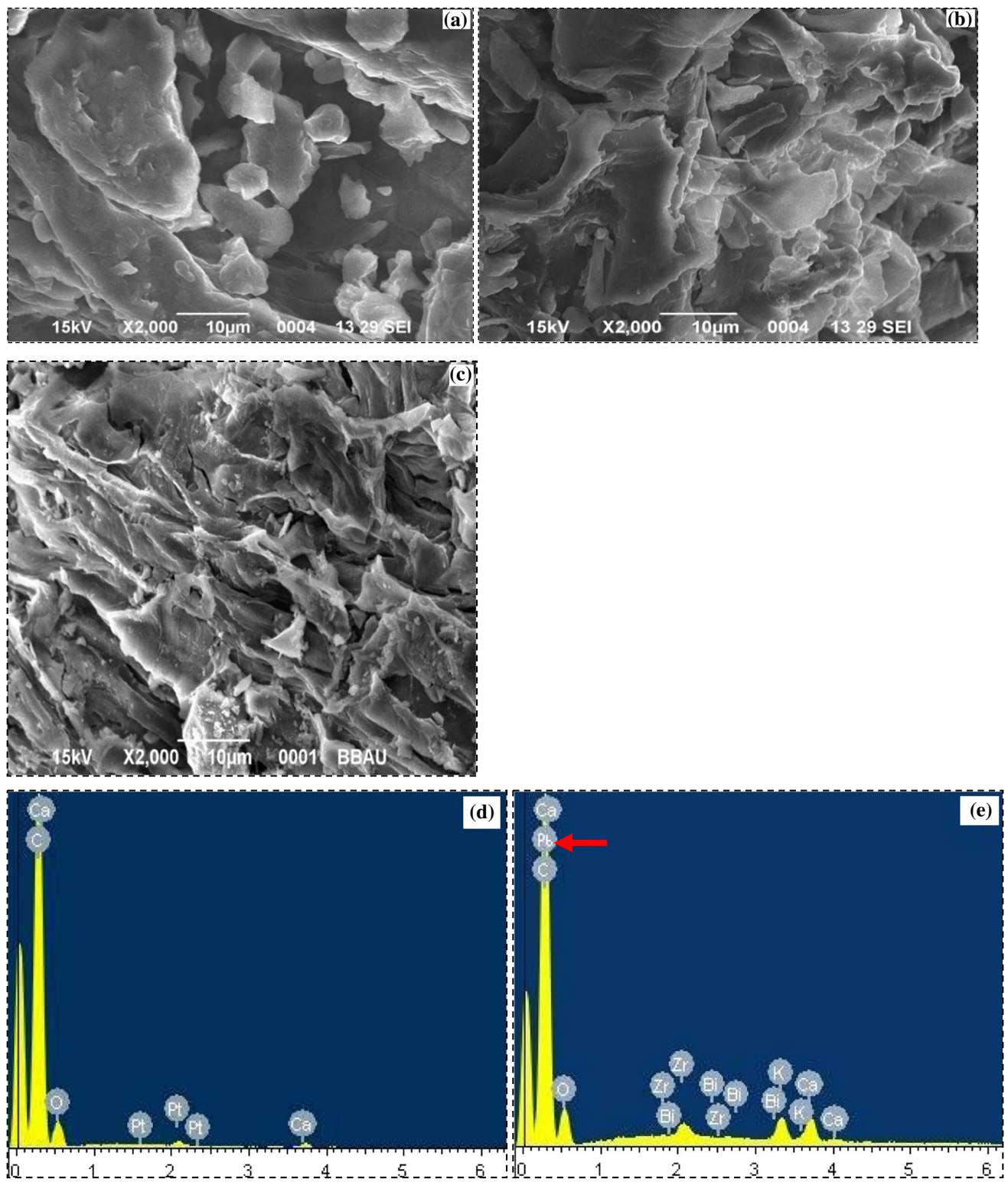


Fig. 2 SEM images of: **a** bagasse, **b** bagasse biochar, **c** lead (Pb²⁺)-loaded bagasse biochar; EDX spectrum of **d** bagasse biochar and **e** lead (Pb²⁺) adsorbed

in Fig. 3. The broad peaks between 3846 and 3438 cm^{-1} show the presence of $-\text{OH}$ stretching vibrations of cellulose, pectin and lignin in all the three spectra (Guo et al. 2008; Reddy et al. 2014). After thermal treatment, most of the major peaks were disappeared except $-\text{CH}$ stretching at 2925.3 cm^{-1} , $\text{C}=\text{O}$ stretch in ketones represented by broad peak at 1711 cm^{-1} , $\text{C}=\text{C}$ stretch in alkenes and $\text{C}=\text{O}$ stretch in secondary amides represented by a sharp peak at 1631 cm^{-1} . The stretching of the chemical bonds is marked by the higher carbon content as well as the organic matter (Abdelhafez and Li 2016). After the adsorption of Pb^{2+} the peaks were shifted to 1629.7, 1441.67 and 874.97 cm^{-1} representing $\text{C}=\text{O}$ stretching at $\text{C}-\text{N}$ stretch in primary amides at $\text{C}-\text{H}$ and CH_2 deformations, respectively. Conversion of secondary amide to primary amide and $-\text{CH}$ to $\text{C}=\text{C}$ is evident of formation and dissociation of bonds and groups through ion exchange or some other mechanisms (Kim et al. 2015). The shift in the functional groups between non-treated and treated adsorbent suggests that the adsorption of Pb^{2+} might be facilitated by the process of chemisorption resulting in binding of the metal by the nucleophilic functional groups resulting in the formation of metal complex. This process also supported the adsorption of Pb^{2+} onto the bagasse biochar.

Surface acidic groups

The surface acidic group concentrations of bagasse biochar are represented in Fig. 4. The total concentration of surface acidic groups was 7.033 mol g^{-1} . The carboxylic acidic functional groups occupied maximum concentration of 5.15 mol g^{-1} in comparison with other phenolic (1.283 mol g^{-1}) and lactonic (0.601 mol g^{-1}) acidic groups. The results of the Boehm titration indicated majority of carboxylic acidic groups occupying 72.963% of total surface acidic groups, followed by lactonic (18.182%) and phenolic (8.855%) groups. These results were in good agreement with those of FTIR analysis, explained earlier.

Effect of pH

The effect of pH on concentration of Pb^{2+} is presented in Fig. 5. pH is an important controlling parameter in adsorption process as it determines the surface charge of adsorbent, degree of ionization of the adsorbate and extent of dissociation of functional groups present on active sites (Yang and Cui. 2013; Salam et al. 2011). Thus, the effect of H^+ ions concentration in the battery manufacturing industry effluent was studied at different pHs at optimized dosage (5.0 g l^{-1}) and contact time (140 min). Above pH 7, precipitation of oxides of Pb^{2+} was formed; therefore, the study was confined to pH range of 2.0–6.0 (Basu et al. 2017). The optimum pH for the removal of Pb^{2+} was found to be 5. As the pH of the

effluent was increased from 2 to 5, the adsorption capacity of the adsorbent also increased from 3.34 to 3.68 mg g^{-1} . In acidic medium, availability of binding sites increases and removal of H^+ ions in the solution facilitates it being replaced by Pb^{2+} which is termed as chelation. Since Pb has +2 charges, two carbon atoms are involved in chelating/binding of the metal resulting in the formation of metal complex. This may also be the probable reason for the shift in the IR spectra too. At lower pH, there was Coulombic repulsion between positively charged binding sites and cations which suppressed the removal rate, further (Liu and Zhang 2009). The result is in agreement with previous studies for the removal of Pb^{2+} by bamboo charcoal (Wang et al. 2012), dried water hyacinth (Ibrahim et al. 2012), rapeseed oil cake (Uçar et al. 2015) and strain of *Alcaligenes* sp. (Jin et al. 2017).

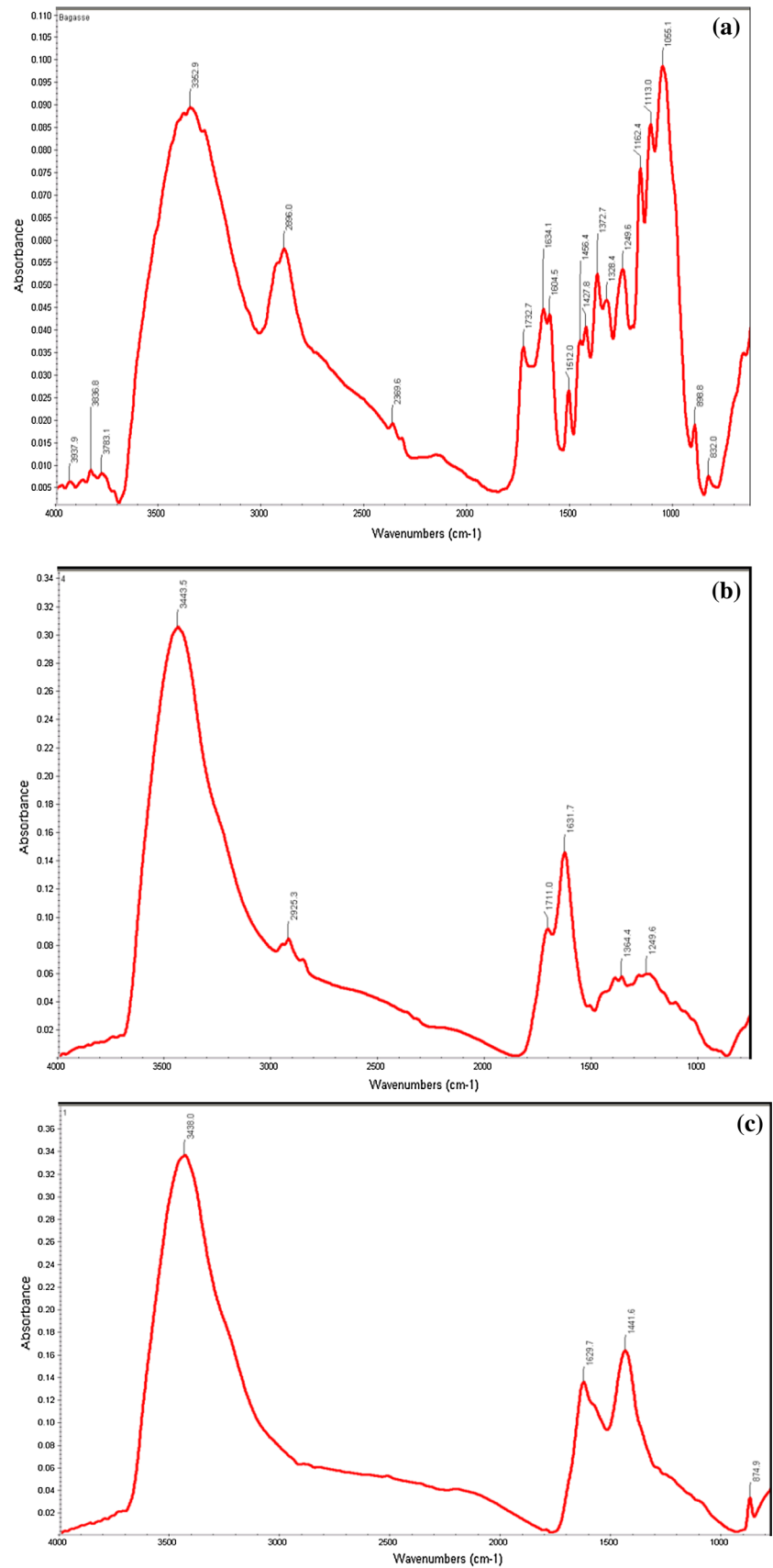
Effect of adsorbent dosage

The effect of adsorbent dosages on the concentration of Pb^{2+} in battery manufacturing industry effluent is presented in Fig. 5. The experiments were carried out at different dosages ranging from 2.5 to 5 g l^{-1} . For convenience in presenting the data, the initial dose was chosen as 2.5 g l^{-1} since the removal rate was found to decrease from 66.696 to 64.345% and so on, when the dosage was reduced from 2.5 to lesser. But, when the amount of adsorbent dosage was increased further from 2.5 to 5.0 g l^{-1} , the removal percentage increased from 66.696 to 75.376%. It can be justified by the fact that increasing dose upsurges the number of binding sites for the metal (Gil et al. 2018). The optimum dose for maximum removal of Pb^{2+} from effluent was recorded 5.0 g l^{-1} . Moreover, when dosage was increased further, removal rate decreased due to overloading and intracellular dissociation phenomenon, which affected the binding capacity of the surface groups (Zhao et al. 2017). These results were in agreement with previous studies performed on many other adsorbents for different metals including Pb^{2+} (Oluyemi et al. 2012; Kılıç et al. 2013; Reddy et al. 2014).

Effect of contact time

The contact time also plays a major role in the adsorption of metals from effluent. The effect of contact time on the concentration of Pb^{2+} in the effluent is shown in Fig. 6. The contact time was varied from 20 to 140 min. In initial 20 min about 64.79% of Pb^{2+} was adsorbed, after which the process slowed down and till 140 min the binding sites of the adsorbents became saturated with 75.376% removal of Pb^{2+} . Thus, the optimum time for the removal of Pb^{2+} was 140 min. No further change in the concentration of Pb^{2+} was observed due to exhaustion of the active binding sites. Similar outcomes were also accomplished when adsorbent

Fig. 3 FTIR spectra of: **a** bagasse, bagasse biochar before **b** and after **c** Pb^{2+} adsorption



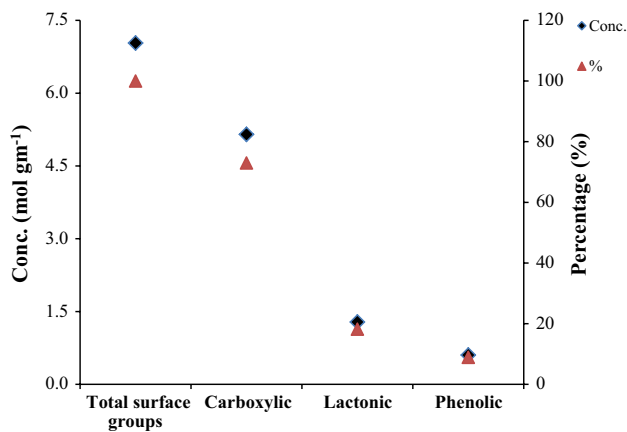


Fig. 4 Surface acidic groups concentration (mol g⁻¹) of bagasse biochar

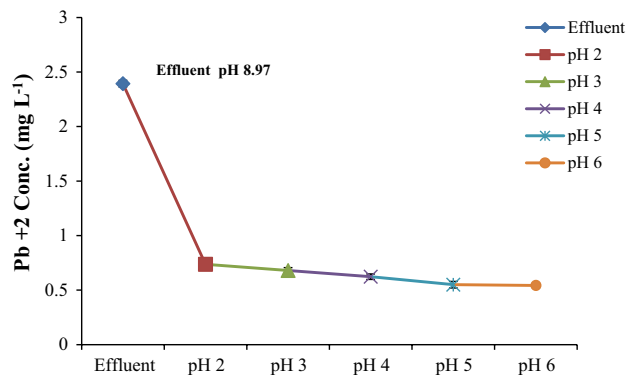


Fig. 5 Effect of different pHs on the concentration of Pb²⁺ in battery manufacturing industry effluent after adsorption at room temperature (25 ± 3 °C) and optimized pH 5, adsorbent dose 5.0 g l⁻¹ and contact time of 140 min (SD shown by error bars)

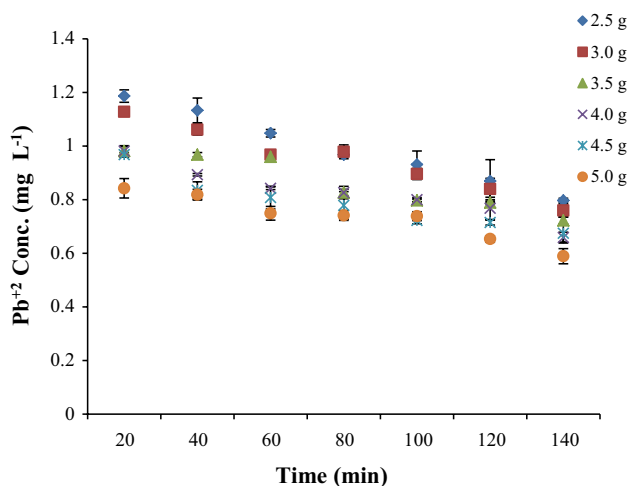


Fig. 6 Effect of time adsorbent dose and contact time lead (Pb²⁺) concentration, at constant temperature (25 ± 3 °C)

dosage and pH were optimized. Moreover, the results are in agreement with Uçar et al. (2015).

Adsorption kinetics

The plots of pseudo-first order and pseudo-second order for the adsorption of Pb²⁺ onto bagasse are presented in Fig. 7. The linear plots of t versus $\log(q_e - q_t)$ and t versus t/q_t offer the pseudo-first- and second-order rate constants K_1 and K_2 , respectively, which are calculated by the slope and intercept. The corresponding values of K_1 , K_2 , q_e and r^2 are represented in Table 3.

According to correlation coefficients (r^2), the correlation coefficients for pseudo-second-order kinetic model were higher than those of the pseudo-first-order model for Pb²⁺. This suggests that the adsorption process followed the pseudo-second-order kinetics, indicating adsorption takes place by chemisorptions (Reddy et al. 2014). The results of the present study are in good agreement with previous studies, which also reported that the adsorption process follows the pseudo-second-order kinetics (Uçar et al. 2015; Ibrahim et al. 2012; Wang et al. 2012).

Adsorption isotherm

Adsorption isotherms are used to describe the adsorption equilibrium for wastewater treatments by providing useful information regarding adsorbent surface (Uçar et al. 2015; Naiya et al. 2009). At equilibrium, battery manufacturing industry effluent was allowed to contact with varying dosages of bagasse biochar to examine the maximum loading capacity of the adsorbent used. Adsorption process was justified by applying linear forms of Langmuir and Freundlich isotherms (Langmuir 1918; Freundlich 1906).

The plots of Langmuir isotherm for $1/q_e$ versus $1/C_e$ and Freundlich isotherm for $\log q_e$ versus $\log C_e$ are presented in Fig. 8. Moreover, values of different parameters for both isotherms and separation factor (R_L) are given in Table 4.

Although there is very less difference between both of the isotherms, the results indicated that in comparison with Freundlich ($r^2 = 0.927$), Langmuir isotherm ($r^2 = 0.9298$) better fitted for the adsorption of Pb²⁺ from battery manufacturing industry effluent. Langmuir model assumes that there were no interactions between solute particles and adsorbent surfaces, and solute particles were distributed in a monolayer carbon surface (Uçar et al. 2015). The monolayer adsorption capacity (q_{max}) of bagasse biochar for the removal of Pb²⁺ from battery manufacturing industry effluent was found to be 12.74 mg g⁻¹. The value of q_{max} was found to be less than previously reported literature; the reason behind this may be the treatment of effluent (with lesser conc. of 2.39 mg l⁻¹ Pb²⁺) than of known solutions of metals (with higher metal

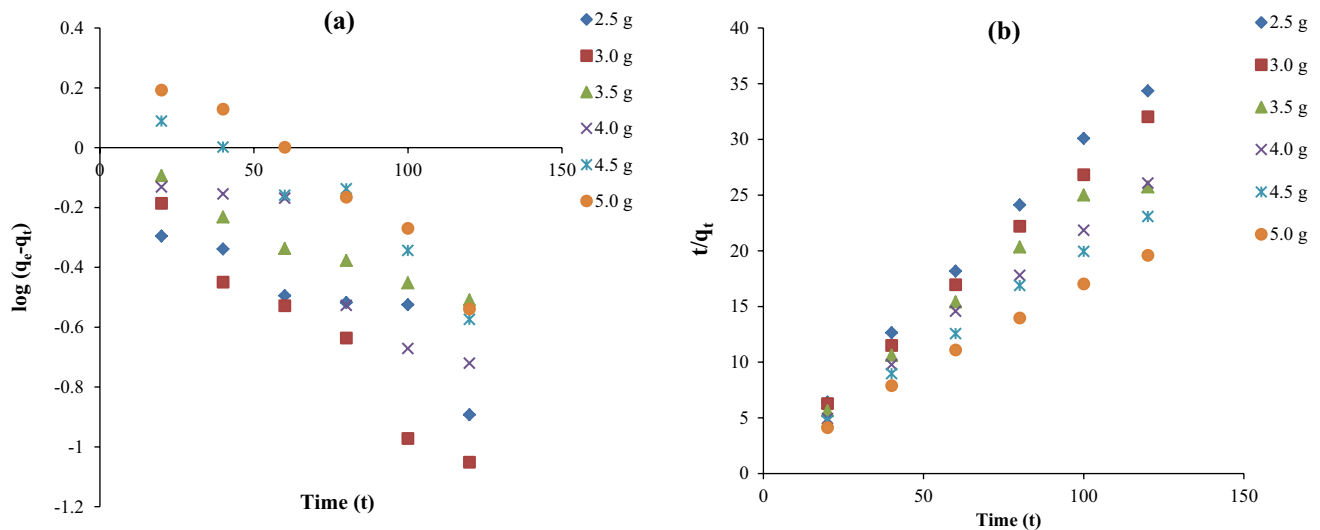


Fig. 7 Role of time **a** pseudo-first-order kinetic plots and **b** pseudo-second-order kinetic plots

Table 3 Pseudo-first-order and pseudo-second-order kinetic constants for sorption of lead (Pb^{2+}) onto bagasse biochar

Parameters	Dosage (g)					
	2.5	3.0	3.5	4.0	4.5	5.0
q_e (exp.) (mg g^{-1})	6.411	5.467	4.792	4.353	3.834	3.621
Pseudo-first-order model constants						
q_1 (mg g^{-1})	2.471	1.758	1.227	1.135	1.086	1.432
K_1 (min^{-1})	0.016	0.014	0.014	0.009	0.018	0.012
R^2	0.817	0.963	0.961	0.889	0.925	0.963
Pseudo-second-order model constants						
q_2 (mg g^{-1})*	6.412	5.467	4.792	4.353	3.834	3.621
K_2 ($\text{g}^{-1} \text{mg}^{-1} \text{min}^{-1}$)	15.060	11.474	8.456	24.263	6.586	4.887
r^2	0.997	0.999	0.974	0.996	0.996	0.996
h ($\text{mg g}^{-1} \text{min}^{-1}$)	6.536	5.435	4.831	4.717	3.891	3.546

*Calculated from graph $1/t$ versus $1/q_t$

conc.) containing higher concentrations of it (Reddy et al. 2014; Naiya et al. 2009; Wang et al. 2012).

Further, the feasibility of Langmuir isotherm can also be proved by a dimensionless constant, viz. separation factor or equilibrium parameter separation factor (R_L) (Hall et al. 1966). It is represented as follows

$$R_L = \frac{1}{1 + K_L C_0}$$

where C_0 is initial metal concentration. If the value of R_L is between 0 and 1, then the adsorption is favorable, and if it is higher than 1, then adsorption is unfavorable. If $R_L = 1$, then adsorption is linear, and the $R_L = 0$ indicates irreversible adsorption. In the present study, R_L value was less than 0, i.e., 0.603, showing favorable adsorption of Pb^{2+} onto bagasse biochar.

Desorption and reuse of adsorbent

Desorption process is a reverse process of adsorption and is important to understand its recovering capacity and reusability for commercial application (Zhang et al. 2018). Three acids (HNO_3 , HCl and H_2SO_4) and one base (NaOH) of 0.1 M were used as eluants to assess the desorption process. HNO_3 was found to be the best eluants to desorb about 90.05% of Pb^{2+} from the adsorbent (Fig. 9). The result is in agreement with previous studies done by Naiya et al. (2009) and Mondal (2009).

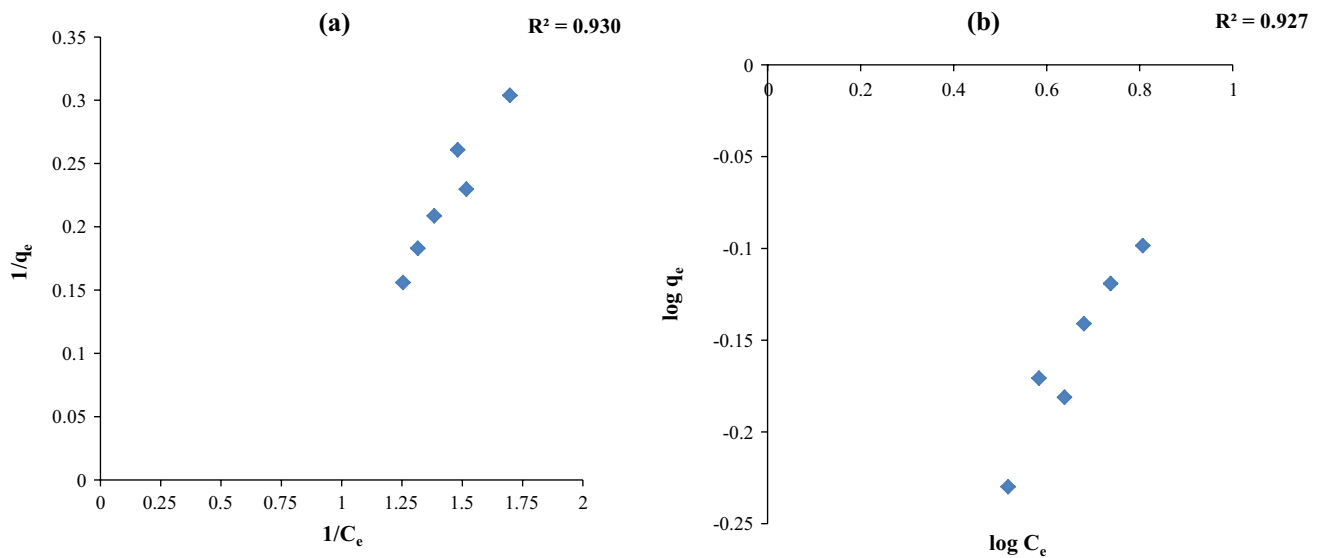


Fig. 8 a Langmuir and b Freundlich isotherm models for adsorption of Pb²⁺ on bagasse biochar

Table 4 Langmuir along with Freundlich isotherm constants and separation factor for the adsorption of Pb²⁺ on bagasse biochar

Langmuir constants		Freundlich constants			Separation factor	
q_{max} (mg g ⁻¹)	b (L mg ⁻¹)	r^2	K_F (mg g ⁻¹)	n	r^2	R_L^*
12.741	4.120	0.930	0.353	2.227	0.927	0.603

*Value is given for optimum dose (5.0 g l⁻¹) and conc. of effluent (2.39 mg l⁻¹)

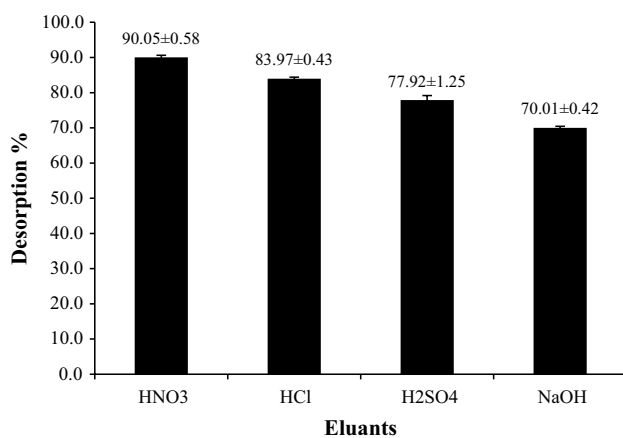


Fig. 9 Desorption efficiency of different eluants for desorption of Pb²⁺ from bagasse biochar ±SD shown by error bar

Conclusions

From different agricultural wastes, bagasse was screened as a potential adsorbent for removing from wastewater of battery manufacturing industry effluent. The adsorption

process was found to be dependent upon the pH of the medium as well as the contact time and dosage. The maximum adsorption capacity was recorded as 12.741 mg g⁻¹ which is good for removing trace amount of metal from wastewater before disposal to the water bodies. The adsorption capacity of bagasse biochar may be increased by modifying it with various physicochemical methods like charring, addition of chemicals. The results concluded that the bagasse may be used as cost-effective adsorbent for the successful removal of different wastewater generating industries. It may also be utilized in the production of commercial bioadsorbents for removing various heavy metals from industrial effluents.

Acknowledgements The authors would like to thank Mr. Shamshad Ahmad, Department of Environmental Science, and Dr. Vertika Shukla, Department of Applied Geology, BBA University, Lucknow, for their help and support.

Open Access This article is distributed under the terms of the Creative Commons Attribution 4.0 International License (<http://creativecommons.org/licenses/by/4.0/>), which permits unrestricted use, distribution, and reproduction in any medium, provided you give appropriate credit to the original author(s) and the source, provide a link to the Creative Commons license, and indicate if changes were made.

References

- Abdelhafez AA, Li J (2016) Removal of Pb(II) from aqueous solution by using biochars derived from sugarcane bagasse and orange peel. *J Taiwan Inst Chem Eng* 61:367–375
- Ahmed TF, Sushil M, Krishna M (2012) Impact of dye industrial effluent on physicochemical characteristics of Kshipa River, Ujjain City, India. *Int Res J Environ Sci* 1:41–45
- Ajenifuja E, Ajao JA, Ajayi EOB (2017) Adsorption isotherm studies of Cu(II) and Co(II) in high concentration aqueous solutions on photocatalytically modified diatomaceous ceramic adsorbents. *Appl Water Sci* 7:3793–3801
- Akpomie KG, Dawodua FA (2015) Physicochemical analysis of automobile effluent before and after treatment with an alkaline-activated montmorillonite. *J Taibah Univ Sci* 9(4):465–476
- Alluri HK, Ronda SR, Settalluri VS, Bondili VS, Suryanarayana V, Venkateshwar P (2007) Biosorption: an eco-friendly alternative for heavy metal removal. *Afr J Biotechnol* 6(11):2924–2931
- Amuda OS, Giwa AA, Bello IA (2007) Removal of heavy metal from industrial wastewater using modified activated coconut shell carbon. *Biochem Eng J* 36:174–181
- Andrade V, Mateus M, Batoréu M, Aschner M, dos Santos AM (2015) Lead, arsenic, and manganese metal mixture exposures: focus on biomarkers of effect. *Biol Trace Elem Res* 166(1):13–23
- APHA (2005) Standard methods for the examination of water and waste water, 21st edn. American Public Health Association, Washington, DC
- Babel S, Kurniawan TA (2003) Low-cost adsorbents for heavy metals uptake from contaminated water: a review. *J Hazard Mater B* 97:219–243
- Banerjee K, Ramesh ST, Nidheesh PV, Bharathi KS (2012) A novel agricultural waste adsorbent, watermelon shell for the removal of copper from aqueous solutions. *Iran J Energy Environ* 3:143–156
- Basu M, Guha AK, Ray L (2017) Adsorption of lead on Cucumber peel. *J Clean Prod* 151:603–615
- BIS (2012) Indian standards specifications for drinking water. IS:10500, Bureau of Indian Standards, New Delhi. <http://cgwb.gov.in/Documents/WQ-standards.pdf>
- Boehm HP, Diehl E, Heck W, Sappok R (1964) Surface oxides of carbon. *Angewandte Chem Int Ed* 3:669–677
- Buasri A, Nattawut C, Tapang K, Jaroensin S, Panphrom S (2012) Equilibrium and kinetic studies of biosorption of Zn(II) ions from wastewater using modified corn cob. *APCBEE Procedia* 3:60–64
- Cheraghi M, Sobhanardakani S, Zandipak R, Lorestani B, Merrikhpour H (2015) Removal of Pb(II) from aqueous solutions using waste tea leaves. *Iran J Toxicol* 9(28):1247–1253
- Doke KM, Khan EM (2017) Equilibrium, kinetic and diffusion mechanism of Cr(VI) adsorption onto activated carbon derived from wood apple shell. *Arab J Chem* 10(Supplement 1):S252–S260. <https://doi.org/10.1016/j.arabj.2012.07.031>
- Ehrampoush MH, Miria M, Salmani MH, Mahvi AH (2015) Cadmium removal from aqueous solution by green synthesis iron oxide nanoparticles with tangerine peel extract. *J Environ Health Science Eng* 13(1):1
- Fernandez ME, Nunell GV, Bonelli PR, Cukiermen AL (2014) Activated carbon developed from orange peels: batch and dynamic competitive adsorption of basic dyes. *Ind Crops Prod* 62:437–445
- Freundlich H (1906) Adsorption in solutions (57). *Z Phys Chem Germany* 385–470
- Gardare VN, Yadav S, Avhad DN, Rathod VK (2015) Preparation of adsorbent using sugarcane bagasse by chemical treatment for the adsorption of methylene blue. *Desalin Water Treat.* <https://doi.org/10.1080/19443994.2014.967727>
- Gil A, Amiri MJ, Javad M, Abedi-Koupai J (2018) Adsorption/reduction of Hg(II) and Pb(II) from aqueous solutions by using bone ash/nZVI composite: effects of aging time, Fe loading quantity and co-existing ions. *Environ Sci Pollut Res* 25:2814–2829
- Guo X, Zhang S, Shan X (2008) Adsorption of metal ions on lignin. *J Hazard Mater* 151:134–142
- Hall KR, Eagleton LC, Acrivos A, Vermeulen T (1966) Pore- and solid-diffusion kinetics in fixed-bed adsorption under constant pattern conditions. *Ind Eng Chem Fundam* 5:212–223
- Ho YS, McKay G, Wase DJ, Foster CF (2000) Study of the sorption of divalent metal ions on to peat. *Adv Sci Technol* 18:639–650
- Ibrahim HS, Ammar NS, Ibrahim M (2012) Removal of Cd(II) and Pb(II) from aqueous solution using dried water hyacinth as a biosorbent. *Spectrochim Acta A Mol Biomol Spectrosc* 96:413–420
- Jin Y, Yu S, Teng C, Song T, Dong L, Liang J, Bai X, Xu X, Qu J (2017) Biosorption characteristic of *Alcaligenes* sp. BAPb.1 for removal of lead(II) from aqueous solution. *3. Biotech* 7:123
- Joseph O, Rouez M, Métivier-Pignon H, Bayard R, Emmanuel E, Gourdon R (2009) Adsorption of heavy metals on to sugar cane bagasse: improvement of adsorption capacities due to anaerobic degradation of the biosorbent. *Environ Technol.* <https://doi.org/10.1080/09593330903139520>
- Kılıç M, Kırbyık Ç, Çepelioğullar Ö, Pütün AE (2013) Adsorption of heavy metal ions from aqueous solutions by bio-char, a by-product of pyrolysis. *Appl Surf Sci* 283:856–862
- Kim N, Park M, Park D (2015) A new efficient forest biowaste as biosorbent for removal of cationic heavy metals. *Bioresour Technol* 175:629–632
- Kong Z, Li X, Tian J, Yang J, Sun S (2014) Comparative study on the adsorption capacity of raw and modified litchi pericarp for removing Cu(II) from solutions. *J Environ Manag* 134:109–116
- Lagergren S (1898) *Kungl. Svenska Vetenskapakad Handl* 24:1–39
- Laidlaw MAS, Filoppelli G, Mielke H, Gulson B, Ball AS (2017) Lead exposure at firing ranges—a review. *Environ Law.* <https://doi.org/10.1186/s12940-017-0246-0>
- Langmuir I (1918) The adsorption of gases on plane surfaces of glass, mica and platinum. *J Am Chem Soc* 4(9):1361–1403
- Li J, Zheng L, Liu H (2017) A novel carbon aerogel prepared for adsorption of copper(II) ion in water. *J Porous Mater* 24:1575–1580
- Liu Z, Zhang FS (2009) Removal of lead from water using biochars prepared from hydrothermal liquefaction of biomass. *J Hazard Mater* 167:933–939
- Liu B, Chen W, Peng X, Cao Q, Wang Q, Wang D, Meng X, Yu G (2016) Biosorption of lead from aqueous solutions by ion-imprinted tetra ethylene pentamine modified chitosan beads. *Int J Biol Macromol* 86:562–569
- McKay G, Ho YS (1999) Pseudo-second-order model for sorption processes. *Process Biochem* 34:451
- Mehmood S, Rizwan M, Bashir S, Ditta A, Aziz O, Yong LZ, Dai Z, Akmal M, Ahmed W, Adeel M, Imtiaz M, Tu S (2017) Comparative effects of biochar, slag and Ferrous–Mn ore on lead and cadmium immobilization in soil. *Bull Environ Contam Toxicol.* <https://doi.org/10.1007/s00128-017-2222-3>
- Mondal MK (2009) Removal of Pb(II) ions from aqueous solution using activated tea waste: adsorption on a fixed-bed column. *J Environ Manag* 90:3266–3271
- Naiya TK, Bhattacharya AK, Das SK (2009) Adsorption of Cd(II) and Pb(II) from aqueous solutions on activated alumina. *J Colloid Interface Sci* 333:14–26
- Nguyen TAH, Ngo HH, Guo WS, Zhang J, Liang S, Yue QY, Li Q, Nguyen TV (2013) Applicability of agricultural waste and by-products for adsorptive removal of heavy metals from wastewater: review. *Bioresour Technol* 148:574–585

- Oickle AM, Goertzen SL, Hopper KR, Abdalla YO, Andreas HA (2010) Standardization of the Boehm titration: part II. Method of agitation, effect of filtering and dilute titrant. *Carbon* 48:3313–3322
- Oluyemi EA, Adeyemi AF, Olabanji IO (2012) Removal of Pb²⁺ and Cd²⁺ ions from wastewaters using palm kernel shell charcoal (pksc). *Res J Eng Appl Sci* 1(5):308–313
- Petrović M, Šoštarić T, Stojanović M, Petrović J, Mihajlović M, Čosović M, Stanković (2017) Mechanism of adsorption of Cu²⁺ and Zn²⁺ on the corn silk (*Zea mays* L.). *Ecol Eng* 99:83–90
- Poonam, Kumar M (2018) Efficiency of sweet lemon (*Citrus limetta*) biochar adsorbent for removal of chromium from tannery effluent. *Indian J Environ Prot* 38(3):246–256
- Rangabhashiyam S, Selvaraju N (2015) Adsorptive remediation of hexavalent chromium from synthetic wastewater by a natural and ZnCl₂ activated *Sterculia guttata* shell. *J Mol Liq* 207:39–49
- Reddy NA, Lakshmiopathy R, Sarada NC (2014) Application of *Citrus lanatus* rind as biosorbent for removal of trivalent chromium from aqueous solution. *Alex Eng J* 53:969–975
- Renner R (2010) Exposure on tap: drinking water as an overlooked source of lead. *Environ Health Perspect* 118:A68–A72
- Saad SA, Isa KM, Bahari R (2010) Chemically modified sugarcane bagasse as a potentially low-cost biosorbent for dye removal. *Desalination* 264(1–2):123–128
- Said AE-AA, Soliman AS, El-Hafez AAA, Goda MN (2013) Application of modified bagasse as a biosorbent for reactive dyes removal from industrial wastewater. *J Water Resour Prot* 5:10–17
- Saka C, Şahin Ö, Demir H, Kahyaoğlu M (2011) Removal of lead(II) from aqueous solutions using pre-boiled and formaldehyde-treated onion skins as a new adsorbent. *Sep Sci Technol* 46(3):507–517
- Salam OEA, Reiad NA, ElShafei MM (2011) A study of the removal characteristics of heavy metals from wastewater by low-cost adsorbents. *J Adv Res* 2:297–303
- Salmani MH, Abedi M, Mozaffari SA, Sadeghian HA (2017) Modification of pomegranate waste with iron ions a green composite for removal of Pb from aqueous solution: equilibrium, thermodynamic and kinetic studies. *AMB Express* 7:225. <https://doi.org/10.1186/s13568-017-0520-0>
- Solum MS, Pugmire RJ, Jagtoyen M, Derbyshire F (1995) Evolution of carbon structure in chemically activated wood. *Carbon* 33:1247–1254
- Taha G, Arifien A, El-Nahas S (2011) Removal efficiency of potato peels as a new biosorbent material for uptake of Pb(II) Cd(II) and Zn(II) from their aqueous solutions. *J Solid Waste Technol Manag* 37(2):128–140
- Tahir H, Sultan M, Akhtar N, Hameed U, Abid T (2016) Application of natural and modified sugar cane bagasse for the removal of dye from aqueous solution. *J Saudi Chem Soc* 20:S115–S121
- Trans VH, Tran LD, Nguyen TN (2010) Preparation of chitosan/magnetite composite beads and their application for removal of Pb(II) and Ni(II) from aqueous solution. *Mater Sci Eng C* 30:304–310
- Uçar S, Erdem M, Tay T, Karagö S (2015) Removal of lead(II) and nickel(II) ions from aqueous solution using activated carbon prepared from rapeseed oil cake by Na₂CO₃ activation. *Clean Technol Environ Policy* 17:747–756. <https://doi.org/10.1007/s10098-014-0830-8>
- Venkatesha NJ, Bhat YS, Prakash BSJ (2016) Volume accessibility of acid sites in modified montmorillonite and triacetin selectivity in acetylation of glycerol. *Appl Catal A Gen* 496:51–57
- Wang J, Chen C (2009) Biosorbents for heavy metals removal and their future. *Biotechnol Adv* 27:195–226
- Wang Y, Wang X, Wang X, Liu M, Yang L, Wu Z, Xia S, Zhao J (2012) Adsorption of Pb(II) in aqueous solutions by bamboo charcoal modified with KMnO₄ via microwave irradiation. *Colloids Surf A* 414:1–8
- Xu X, Cao X, Zhao L, Wang H, Yu H, Gao B (2013) Removal of Cu, Zn, and Cd from aqueous solutions by the dairy manure-derived biochar. *Environ Sci Pollut Res* 20:358–368
- Yang X, Cui X (2013) Adsorption characteristics of Pb(II) on alkali treated tea residue. *Water Resour Ind* 3:1–10
- Zhang X, Tong J, Hu XB, Wei W (2018) Adsorption and desorption for dynamics transport of hexavalent chromium Cr(VI) in soil column. *Environ Sci Pollut Res* 25:459–468
- Zhao W, Zhou T, Zhu J, Sun X, Xu Y (2017) Adsorption of cadmium ions using the bioadsorbent of *Pichia kudriavzevii* YB5 immobilized by polyurethane foam and alginate gels. *Environ Sci Pollut Res*. <https://doi.org/10.1007/s11356-017-0785-5>

Publisher's Note Springer Nature remains neutral with regard to jurisdictional claims in published maps and institutional affiliations.